A kinematic wave model in Lagrangian coordinates incorporating capacity drop: application to homogeneous road stretches and discontinuities

Kai Yuan*, Victor L. Knoop, and Serge P. Hoogendoorn

Department of Transport and Planning, Delft University of Technology, Delft, The Netherlands

Abstract

On freeways, congestion always leads to capacity drop. This means the queue discharge rate is lower than the pre-queue capacity. Our recent research findings indicate that the queue discharge rate increases with the speed in congestion, that is the capacity drop is strongly correlated with the congestion state. Incorporating this varying capacity drop into a kinematic wave model is essential for assessing consequences of control strategies. However, to the best of authors' knowledge, no such a model exists. This paper fills the research gap by presenting a Lagrangian kinematic wave model. "Lagrangian" denotes that the new model is solved in Lagrangian coordinates. The new model can give capacity drops accompanying both of stop-and-go waves (on homogeneous freeway section) and standing queues (at nodes) in a network. The new model can be applied in a network operation. In this Lagrangian kinematic wave model, the queue discharge rate (or the capacity drop) is a function of vehicular speed in traffic jams. Four case studies on links as well as at lane-drop and on-ramp nodes show that the Lagrangian kinematic wave model can give capacity drops well, consistent with empirical observations.

Keywords: Traffic flow, Kinematic wave model, Capacity drop, Lagrangian coordinates

*Corresponding author

Email address: K.Yuan@tudelft.nl (Kai Yuan)

1. Introduction

Researchers have devoted much effort to finding solutions to congestion problems. The dynamic traffic operation is possibly one of the most cost-effective strategies. Empirical research provides theoretical bases for promising freeway operations. One of those most crucial empirical findings is the capacity drop phenomenon, which is confirmed empirically in [1], [2].

Once congestion occurs on a freeway, the flow downstream of a traffic jam is lower than the pre-queue capacity. This phenomenon is called the capacity drop. The maximum flow downstream of the jam is called the queue discharge rate. We divide congestion into two categories: stop-and-go waves which propagate upstream with both congestion fronts, and standing queues, whose heads are fixed at bottlenecks. In this research, this division in congestion is duo to the difference in modeling traffic flow on links and nodes.

Incorporating the capacity drop into traffic flow models is crucial for the evaluation of dynamic traffic operations, as argued in [3]. Traffic delays strongly depend on the capacity drop. A model which does not include the capacity drop cannot show benefits obtained from some traffic management strategies (e.g., on-ramp metering strategy). Following earlier works on the empirical observations on the capacity drop, we argue that a model that well incorporates the capacity drop should (i) give a queue discharge rate reduction from the pre-queue capacity and (ii) be able to produce a relation between the queue discharge rate and the speed in congestion, see Figure 1. The relation is presented in [4] with loop detector data collected on freeway A4 and A12 in the Netherlands. Yuan et al. [5] argue that this relation is a result of intra-driver variation mechanism. Giving those two phenomena are relevant for traffic flow models because the accuracy of the reproduced capacity drop influences the values of control variables and even the strategy performances.

The aim of this paper is to incorporate the capacity drop into a macroscopic traffic flow model for traffic operations. A macroscopic traffic flow model is preferred due to its analytical properties. For instance, solutions to macroscopic models are frequently described as closed-form expressions, and are deterministic [6]. Nowadays researchers frequently use second order models to simulate the traffic state evolution on freeways, such as in [7], [8]. The second order model has the ability of giving capacity drop. However, the improved accuracy of the second order model comes at a cost of complexity

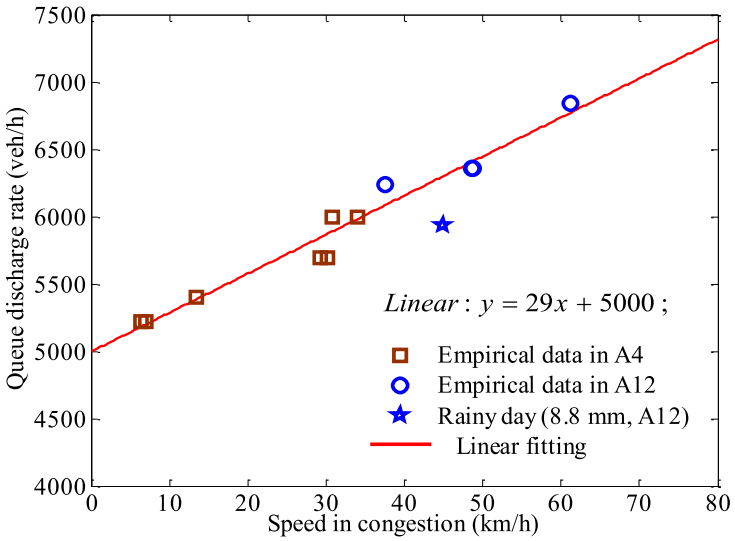

Figure 1: Empirical data showing a relation between the speed in congestion and the queue discharge rate [4]

(e.g., more model parameters) and assumptions. And the second order model can result in negative flow and fast characteristic wave speed. For details, we refer to [9]. By contrast, these issues do not occur in a first order model. Hence, we argue that it is preferred to incorporate the capacity drop into the kinematic wave model.

Earlier works have tried some approaches to capture the capacity drop in the kinematic wave model, e.g., a discontinuous fundamental diagram [10]. However, firstly the discontinuous fundamental diagram will result in infinite shock wave speed and characteristic wave speed, as argued in [11]. Secondly, the discontinuity obtained from empirical data could be a result of non-stationary traffic [12]. Therefore, we believe that it is best to use a continuous fundamental diagram rather than a discontinuous one.

Some efforts have been made, with continuous fundamental diagram, to capture capacity drop in the kinematic wave model. Generally, those efforts are to revise the demand or supply function of cells in the vicinity of congestion. Maria et al. [13] reduce the supply of the immediate downstream cell of congestion by introducing an auxiliary variable illustrating the maximum flow for each cell. Srivastava et al. [14] assume two values of capacity. If the cell is congested during the last time step, the lower-value capacity is used to restrict the supply; or the other higher value is the maximum

supply. Alvarez-Icaza and Islas [15] apply a hysteresis cycle to decide the supply function which is related to the wave speed. But in these works, the capacity drop magnitude is fixed, independent from the congestion states. They cannot reproduce the relation between the queue discharge rate and the congested state.

Some works take account of bounded acceleration effects for giving capacity drop. Literature [16, 17] show that when the density exceeds the critical density, the bounded acceleration effects modify the constant demand to a negative function of density. Combining the LWR-BA model, a bounded acceleration Lighthill-Whitham-Richards (LWR) model by [16, 17], and a node model proposed by Lebacque [18], can give capacity drop as a result of bounded traffic acceleration in the LWR framework [19, 20]. However, this LWR-BA model cannot give queue discharge rate reductions of stop-and-go waves on homogeneous road sections where the node model should be absent.

Some other works consider lane changing to give capacity drop. Muralidharan and Horowitz [21] decrease the supply function at merge cells with a weaving parameter. The weaving parameter illustrates that the merging behavior from the on-ramp occupy more spacing than vehicles from the upstream cell. This concept is similar to the empirical observation in [14]. Moreover, some contributions combine the bounded acceleration and lane changing effects for reproducing the capacity drop (e.g., Roncoli et al. [22], Srivastava and Jin [23], Kontorinaki et al. [24]). Those works let the demand decrease as the over-critical density increases. However, they deal with lane changing effects in different ways. Roncoli et al. [22] present a multi-lane model, giving both of longitudinal and lateral behavior and dividing a multi-lane freeway into different groups of segment-lanes. The flow into and out of each cell in each lane is computed. Srivastava and Jin [23] use a concept of perceived density which is higher than the actually density, that origins from an assumption that the lane changing contribute to the density on both of original and target lanes. Kontorinaki et al. [24] give more capacity to merge cells by modifying supply function to allow a density at the merge cells higher than the critical density. One drawback of those works considering merging, except [22], is that the outflow of stop-and-go waves on homogeneous road sections equals to the free-flow capacity. In [22], lane changing on homogeneous road sections is possible, but the complexity can increase in both of simulations and calibrations, due to a large number of parameters and the grouping of segment-lanes.

To the best knowledge of authors, until now no existing kinematic wave

model can capture the two crucial features, and at the same time keep the simplicity of the kinematic wave model. This paper fills in this research gap. In this contribution, we proposed an extended kinematic wave model in Lagrangian coordinates which can incorporate capacity drop.

The approach we use is to apply a hysteresis loop for the incorporation of capacity drop. For the introduction of the hysteresis loop, we refer to [25]. Some behavioral interpretations of the hysteresis loop are given in [26, 27]. We divide the congested branch in the fundamental diagram into acceleration and deceleration branches. A clockwise hysteresis circle in the flow-density fundamental diagram (i.e., the acceleration branch is below the deceleration one) is utilized to describe the process of passing through traffic congestion. The deceleration branch is fixed, overlapping with the original triangular fundamental diagram. So the traffic state evolution at the upstream front of jams is the same as the original kinematic wave model. But the shock wave speed of the acceleration branch is a function of the congestion states. The acceleration and deceleration branch intersect each other at the congested state. We express the model in Lagrangian coordinates because the Lagrangian formulation can show more efficiency than the Eulerian coordinates in applications (e.g. traffic state estimation [28]). In Lagrangian coordinates, traffic characteristics only move in one direction (upwind) to followers independent of traffic conditions. The simplified solution to the Lagrangian formulation of kinematic wave model is called upwind method. In a preliminary work [29], we present some concepts of this work. However, the solutions proposed in [29] can only be applied to homogeneous freeway sections, which considerably limits the application of the new Lagrangian kinematic wave model. In this paper, we generalize the work in [29] to fully present the Lagrangian kinematic wave model and particularly show how to solve it at lane-drop and on-ramp nodes in Lagrangian coordinates. The proposed solutions at nodes extend the ability of the model to model traffic in a network, which is relevant and necessary for traffic simulations and control evaluations.

The remainer of this contribution is set up as follows. Section 2 proposes the new kinematic wave model and its solutions in Lagrangian coordinates. Section 4 presents the simulation setting and simulation results, followed by Section 5 drawing conclusions.

2. Model Formulation

This section firstly describes the principles of the extended kinematic wave model (Section 2.1), which is presented in Eulerian coordinates for a easy access. We reformulate the new kinematic wave model in Lagrangian coordinates in Section 2.2, since this gives more accurate results with less numerical errors.

2.1. Principles

On a homogeneous freeway without entering or exiting traffic, there is a conservation law of vehicles. We express the conservation law in terms of an equation relating the traffic flow q, speed v and density ρ on a road section, shown as (1) which is also called the conservation equation.

$$\frac{\partial \rho}{\partial t} + \frac{\partial q}{\partial x} = 0 \tag{1}$$

t is the time and x is the location. In equilibrium states, traffic flow, density and speed follow:

$$v(x,t) = \frac{q(x,t)}{\rho(x,t)} \tag{2}$$

Except the conservation law, the other part of the kinematic wave model is the fundamental diagram. In the Cell Transmission model, which does not give capacity drop, the fundamental diagram is a triangular flow-density relation with a free-flow branch and a congestion branch. To integrate the capacity drop, we add acceleration branches to the triangular flow-density fundamental diagram, which lies below the congestion branch. The congestion branch and the acceleration branch form a clockwise hysteresis loop in the flow-density diagram, as shown in Figure 2(a). When vehicles accelerate from congestion, the fundamental flow-density relation follows the acceleration branch which is shown as a dashed line in Figure 2(a). In other words, when the speed remains the same or decreases, the fundamental relation will follow the congestion branch in the triangular fundamental diagram, see the solid line in Figure 2(a). Throughout this manuscript, we also call the congestion branch as the deceleration branch, which has a slope $-w$. We use Q to denote the flow-density relation in the deceleration branch, $q = Q(\rho)$, while the acceleration branch is subscripted by a, $q = Q_a(\rho)$.

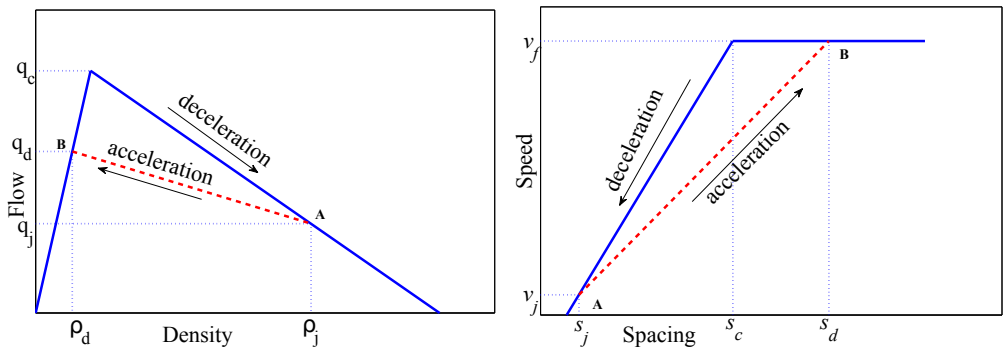

(a) Eulerian coordinates (b) Lagrangian coordinates

Figure 2: Fundamental diagram with capacity drop in (a) Eulerian and (b) Lagrangian coordinates [29]

The acceleration branch intersects with both of the free-flow branch and the congestion branch in the triangular flow-density fundamental diagram at point B and A (see Figure 2(a)), respectively. State B at the free-flow branch indicates a free flow state in the downstream of a vehicular queue. The congested state in the queue is shown as state A. The flow detected at traffic state B is the outflow of congested state A, i.e., the queue discharge rate q_d. The clockwise hysteresis loop indicates that the queue discharge rate q_d is lower than the capacity q_c. That satisfies the definition of the capacity drop.

Traffic state A can be any point in the deceleration branch, indicating different congestion levels. For each state A, there should be an unique acceleration branch which intersects with the deceleration branch at point A. We can have this acceleration branch by calculating the queue discharge rate (corresponding to state B) which is a function of the speed in congested state A, following:

$$q_d(\rho_j) = \min\left(C, \alpha \cdot v_j(\rho_j) + q_0\right) \tag{3}$$

which is the relation between the speed in congestion v_j and the queue discharge rate, as suggested by [4]. C is the pre-queue capacity, which bounds the queue discharge rate in case of over-high queue discharge rates when v_j approaches v_f. In the linear relation in (3), two parameters, α and q_0, are applied. α indicates by how much the traffic jam discharge rate will increase when the speed in the jam grows by 1 unit. q_0 is the queue discharge rate

of wide moving jam in which vehicular speed equals zero. The slope of the acceleration branch $-w_a$, which is a variable, is:

$$w_a(\rho_j) = \frac{q_d(\rho_j) - q_j(\rho_j)}{\rho_d(\rho_j) - \rho_j} \tag{4}$$

ρ_j and $q_j(\rho_j)$ is the density and flow in the congestion state A, respectively. $\rho_d(\rho_j)$ and $q_d(\rho_j)$ are the density and flow in the free-flow state B, respectively. $\rho_d(\rho_j) = q_d(\rho_j)/v_f$ and v_f is the free-flow speed.

With Equation (3), we can have different queue discharge rates (or capacity drop) for different levels of congestion. The corresponding acceleration branch can be found with (4). Once the value for the α and q_0 are calibrated, all acceleration branches have been predefined. Figure 3(a) displays more acceleration branches (shown as light lines), one of which was drawn for each congested state. As shown in Figure 3, we can see that the deceleration branch is fixed while the acceleration branch is variable. The deceleration branch denotes stable equilibrium congested traffic states. In short, our newly proposed kinematic wave model can give both of the capacity drop and the relation between the speed in congestion and the queue discharge rate, as required in the Section 1.

Apart from normal parameters of triangular fundamental diagram, the new kinematic wave model only need to calibrate two parameters, α and q_0. These two parameters have been found in [4]. Note that the assumption of the triangular density-flow fundamental diagram can be relaxed in principle because (3) is independent on the shape of the a continuous density-flow fundamental diagram.

2.2. Formulations in Lagrangian coordinates

In this section, we reformulate our new kinematic wave model in the system of Lagrangian coordinates. The conservation equation which is expressed as (1) in Eulerian coordinate is reformulated as (5):

$$\frac{\partial s(x,t)}{\partial t} + \frac{\partial v(x,t)}{\partial N} = 0 \tag{5}$$

where N is the cumulative number of vehicles, decreasing in space. v is the vehicular speed, which follows a speed-spacing fundamental diagram:

$$v = \begin{cases} V_a(s), & \text{during acceleration} \quad (6) \\ V(s), & \text{otherwise} \quad (7) \end{cases}$$

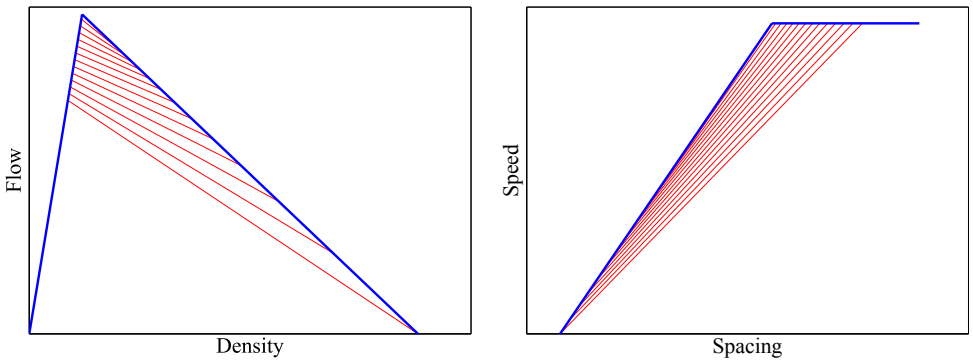

(a) Eulerian coordinates (b) Lagrangian coordinates

Figure 3: Correlations between acceleration branches and congestion in (a) Eulerian and (b) Lagrangian coordinates [29]

with $V_a(s) \neq V(s)$, s is the spacing. The subscript indicates the acceleration branch. The speed-spacing fundamental diagram is shown in Figure 2(b). The bold line is the deceleration branch while the dashed line indicates the acceleration branch. The clockwise hysteresis circle in the flow-density diagram is translated into a counter-clockwise circle in the Lagrangian speed-spacing diagram. The deceleration branch is fixed with a slope:

$$\max \left| \frac{\partial v}{\partial s} \right| = w\rho_{\max} \tag{8}$$

where $\rho_{\max}$ is the maximum jam density, i.e., speed in the queue is zero km/h. The acceleration branch varies depending on the congested state A. Figure 3(b) presents more acceleration branches which are shown as light lines. Corresponding to different congestion states, different acceleration lines are predefined with α and q_0. The maximum speed v_f is the free-flow speed. The minimum spacing is the inverse of the maximum jam density $1/\rho_{\max}$.

The queue discharge rate is formulated into the vehicular spacing downstream of the congestion. The lower the queue discharge rate, the larger the spacing. The coordinates of state B in the Lagrangian coordinate are (s_d, v_f) and

$$s_d = \frac{1}{\rho_d(\rho_j)} \tag{9}$$

s_d is the vehicular spacing in the downstream free flow. With (3), we can rewrite (9):

$$s_d(v_j) = \frac{v_f}{\min(C, \alpha \cdot v_j + q_0)} \tag{10}$$

3. Solutions to the Lagrangian kinematic wave model

To solve the kinematic wave model, this publication applies an upwind method in Lagrangian coordinates. In Lagrangian coordinates, Lagrangian clusters only react to their leading Lagrangian clusters. Characteristics only move upwind to their followers. Only upwind method is needed which results in more efficient simulations [30]. By the contrast, the minimum supply demand method, which is applied in most of LWR models (e.g., the Cell Transmission Model), switches between the upwind and downwind method, that depends on traffic states in the road cells [30]. Characteristics propagate in a switch of downstream (upwind) and upstream (downwind). For more details about the upwind method in the Lagrangian coordinates, we refer to [31], [30], [32]. For more information about the upwind method in Eulerian coordinates, we refer to [33].

This section describes the solutions to the Lagrangian kinematic wave model on links in Section 3.1, followed by Section 3.2 presenting the solutions at nodes. Section 3.3 briefly discuss the numerical diffusion.

3.1. Links

This section firstly describes the upwind method in Lagrangian coordinates on links briefly. Then we adjust the speed updating process in the method for solving the Lagrangian kinematic wave model.

3.1.1. Basic upwind method

Vehicles and time are divided into vehicular groups, which are referred to as Lagrangian clusters in this manuscript, and time steps. Each Lagrangian cluster, indicated by a subscript i, is characterized by three quantities: number of vehicles ΔN, spacing $s(k)$ and speed $v(k)$. k is the time instant, $t = k \cdot \Delta t$, and Δt is the time step.

Lagrangian cluster i follows Lagrangian cluster $i-1$. The upwind method is expressed in time discretization as:

$$s_i(k+1) = s_i(k) + \frac{\Delta t}{\Delta N} \cdot (v_{i-1}(k) - v_i(k)) \tag{11}$$

The numerical scheme (11) is equivalent to the following expression:

$$x_i(k+1) = x_i(k) + v_i(k) \cdot \frac{\Delta t}{\Delta N} \tag{12}$$

which updates the new position x of the Lagrangian cluster i.

For stability and convergence, the time step Δt should satisfy the Courant-Friedrichs-Lewy (CFL) condition as shown in (13):

$$\frac{\Delta N}{\Delta t} \geqslant \max \left| \frac{\partial v}{\partial s} \right| \tag{13}$$

For the interpretation of the CFL condition, we refer to [30]. If the CFL condition is satisfied as an equality, the upwind method can be free of numerical errors [31].

3.1.2. Speed updating process

The Lagrangian cluster speed updating process is presented in Figure 4. V_i^* is the default fundamental speed-spacing relation, following which Lagrangian cluster i updates its speed at present. V_i^* is updated every time step, too. This process firstly updates the Lagrangian cluster's position and spacing. Then, it checks which speed-spacing branch the Lagrangian cluster follows. This checking process is introduced with a dashed rectangle in Figure 4. If $v_i(t) = v_f$, the speed updating process should follow the deceleration branch $V_i^* = V$ (Process 4). If not, firstly the process is going to update the speed with the default speed-spacing relation which has been updated in the last time step. Secondly, we check whether an acceleration branch should be or have been activated. If the acceleration branch has been activated, then the default relation V_i^* remains the same as that in the last time step (Process 1). If the acceleration branch should be but has not been activated yet, then it means $v_i(t)$ is the speed in congestion. The default relation will be updated into an acceleration branch (Process 2). If the acceleration should not be activated, the default relation V_i^* equals to V (Process 3). Except process 1, the rest processes will update the Lagrangian cluster speed following the newly updated speed-spacing relation V_i^*. Process 1 and process 4 only updates speed for one time, while process 2 and process 3 needs to update speed twice. For process 2 and 3, the first speed updating checks whether the cluster is speeding up, and the second speed updating determines by how many the speed should increase.

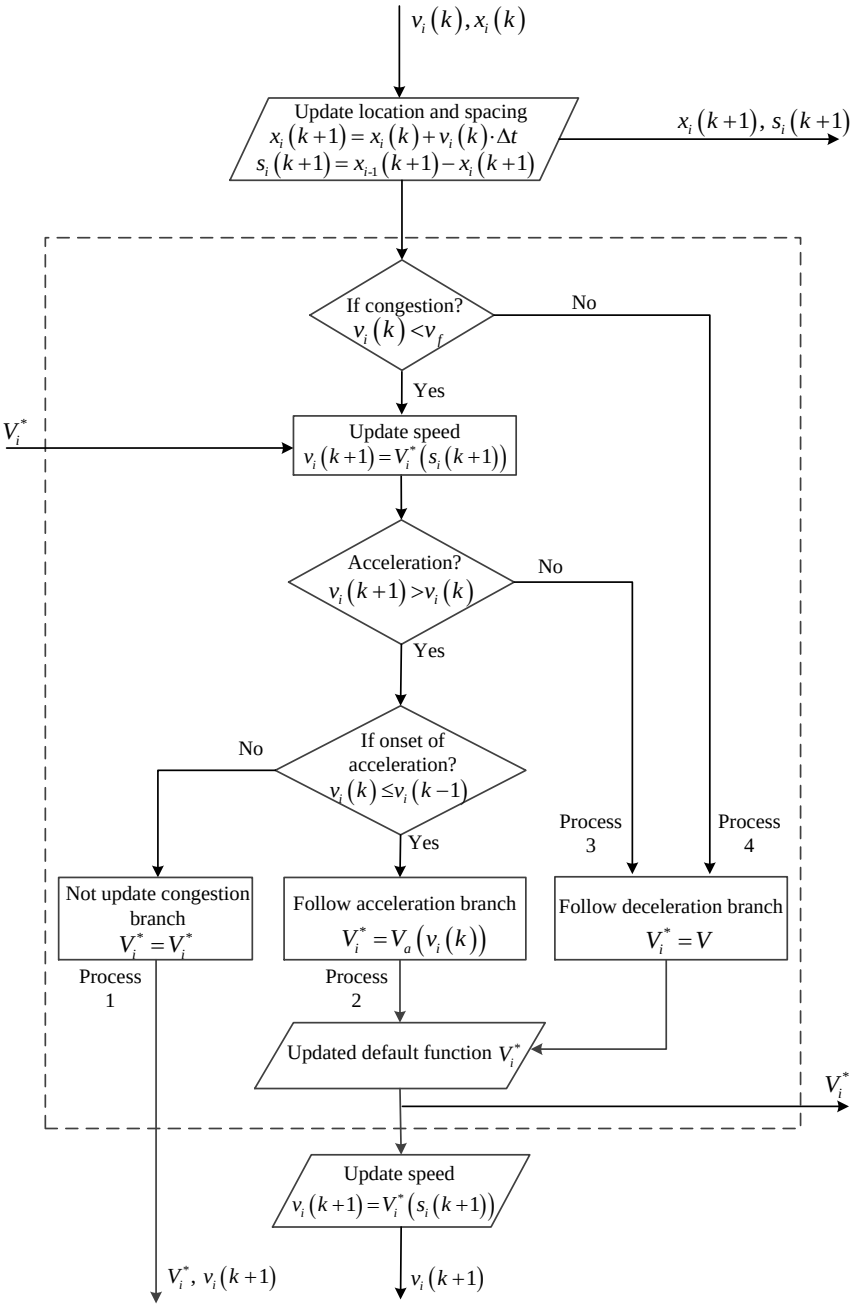

Figure 4: The process of updating Lagrangian cluster speed, part of which is from [29])

3.2. Nodes

Freeways network consist of links and nodes. Section 3.1 only considers links, or homogeneous road sections. This section discusses how to solve the Lagrangian kinematic wave model at nodes. We discuss a lane-drop (Section 3.2.1) and on-ramp (Section 3.2.2) nodes in this work. Van Wageningen-Kessels et al. [30] presents a methodology of modeling nodes using the basic kinematic wave model in Lagrangian coordinates. Based on [30] and [34], this section presents how to model nodes in Lagrangian coordinates when incorporating capacity drops.

3.2.1. Lane-drop nodes

When a Lagrangian cluster reaches a lane-drop node, a change of the fundamental diagram occurs. Usually this change occurs when the Lagrangian cluster passed the node rather than the beginning or end of a time step. This work applies the new fundamental diagram to the Lagrangian cluster at the end of the time step during which the Lagrangian clusters the node. With different fundamental diagrams, the parameters α and q_0 change, accordingly.

Meanwhile, the speed in congestion $v_j(\rho_j)$ does not change. If one Lagrangian cluster passes the lane-drop node during acceleration process (or the Lagrangian cluster keeps accelerating at the end of the time step during which the Lagrangian clusters the node), when drawing the acceleration branch with (10) for the downstream road section, we should still apply the speed in the queue which is in the upstream of the node.

3.2.2. On-ramp nodes

The on-ramp node is a merging node. Without incorporating capacity drops, two issues occur. Firstly, on-ramp nodes add vehicles into the flow on the main road. Secondly, when there is a conflict between the merging Lagrangian cluster and the Lagrangian cluster on the main road, a merging ratio determines which Lagrangian cluster (i.e., the one from the main road or the one from the on ramp) can merge into the main road more easily. Next, both issues are discussed.

For the first issue, Van Wageningen-Kessels et al. [30] address it by modeling that the trajectory of every Lagrangian cluster is continuous. When the number of vehicles on the on-ramp reaches ΔN, the Lagrangian cluster is added to the flow on the freeway. For the second issue, Van Wageningen-Kessels [34] distribute available space between incoming Lagrangian clusters

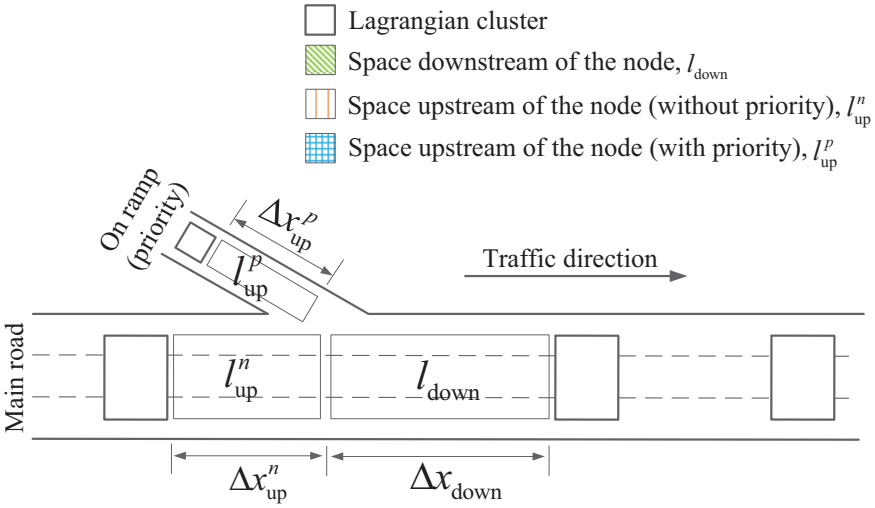

Figure 5: An illustration of available space

on the main road and the on ramp. We briefly present the distributing approach with equations in this section. For more elaborations, we refer to [30] and [34]. In this contribution, the approach applied to solve the Lagrangian kinematic wave model at on-ramp nodes is compared to the contributions in [30] and [34].

In this work, the "space" denotes the room within a certain spacing or the spacing in each lane, that is spacing × number of lanes on one road section. It is the spacing that is used for calculating the speed of the Lagrangian cluster. As illustrated in Figure 5, the available space at the on-ramp node consists of three space: the space on the outgoing link l_{down}, the space upstream of the node on the link with priority l^p_{up} and the space upstream of the node on the other link l^n_{up}. The superscript p indicates the parameter for the Lagrangian cluster with priority while the n denotes the parameter for the Lagrangian cluster without priority. The space l^p_{up} and l^n_{up} are only available to the Lagrangian cluster with and without priority, respectively. The space l_{down} is distributed according to the priority. For the Lagrangian cluster with priority, the solution distributes as much as critical space $\Delta N s^p_c m^p$ to the Lagrangian cluster with priority, including l^p_{up}. s^p_c is the critical spacing on the incoming link with priority. If $l_{\text{down}} + l^p_{\text{up}} < \Delta N s^p_c m^p$, all space $l_{\text{down}} + l^p_{\text{up}}$ is distributed to the Lagrangian cluster with priority. Then, we divide the

distributed space by $\Delta N m^p$ to get the spacing s_i^p, that is:

$$s_i^p = \frac{\max\left(l_{\text{up}}^p, \min\left(\Delta N s_c^p m^p, l_{\text{up}}^p + l_{\text{down}}\right)\right)}{\Delta N m^p} \tag{14}$$

m^p is the number of lanes on the link with priority. m_{down} is the number of lanes on the outgoing link. $l_{\text{up}}^p = \Delta x_{\text{up}}^p m^p$ and $l_{\text{down}} = \Delta x_{\text{down}} m_{\text{down}}$. Set Δx_{up}^p is the distance between the most downstream Lagrangian cluster on the link with priority and the node. Δx_{down} is the distance between the node and the most upstream Lagrangian cluster on the outgoing link, see Figure 5.

The remaining space is distributed to the Lagrangian cluster without the priority. Hence, the Lagrangian cluster without priority gets all the remaining space $l_{\text{up}}^p + l_{\text{up}}^n + l_{\text{down}} - \Delta N m^p s_i^p$. The speed of the Lagrangian cluster without the priority is calculated according to the distributed spacing. The spacing for the Lagrangian cluster without priority equals to the distributed space divided by $\Delta N m^n$. That is, the spacing of the Lagrangian cluster without priority is calculated as follows:

$$s_i^n = \frac{l_{\text{up}}^p + l_{\text{up}}^n + l_{\text{down}} - \Delta N m^p s_i^p}{\Delta N m^n} \tag{15}$$

m^n is the number of lanes on the incoming link without priority. $l_{\text{up}}^n = \Delta x_{\text{up}}^n m^n$ is the available space on the incoming link without priority. Δx_{up}^n is the distance between the most downstream Lagrangian cluster on the link without priority and the node.

The distribution of the priority depends on the merging ratio γ. Priority is given to the on ramp when $N_n/N < \gamma$. Or the main road gains the priority. N_n is the number of Lagrangian clusters from the on ramp within the last n Lagrangian clusters recently passing the node.

After calculating the spacing of each Lagrangian cluster from different upstream links, the Lagrangian kinematic wave model applies the process diagram in Figure 4 to update Lagrangian cluster speed on the main road. Since the fundamental diagram does not change, which is different from the lane-drop node, the queue discharge rate in response to the standing queue can be given accordingly.

3.3. Numerical errors

In the Lagrangian kinematic wave model, a temporary change in the fundamental diagram is caused by a change of traffic situations. The change

of the fundamental diagram indicates that the CFL condition cannot be satisfied as an equality all the time.

When applying the upwind discretization method in the Lagrangian coordinate to solve the kinematic wave model, numerical errors arise inevitably. Without capacity drop, the upwind method can be free of numerical errors by setting an equal sign in CFL condition [31], see (16).

$$\Delta t = \Delta N \cdot \max \left| \frac{\mathrm{d}S(v)}{\mathrm{d}v} \right| \tag{16}$$

$S(v)$ is the inverse of $V(s)$, i.e., $S(v) = V^{-1}(s)$.

However, in the extension the slope of the acceleration branch $V_a(s)$ is smaller than that of the deceleration branch $V(s)$, see Figure 2(b), so:

$$\Delta t < \Delta N \cdot \max \left| \frac{\mathrm{d}S(v)}{\mathrm{d}v} \right| \tag{17}$$

The fact that there is no equal sign in (17) means that when vehicles accelerate from congestion, numerical errors will be inevitable.

4. Simulation

This paper simulates the new kinematic wave model with adaptive capacity drop. The simulation wants to highlight the capability of reproducing the two important phenomena which have been described in Section 1. We present the simulation set-up in Section 4.1 and the simulation results in Section 4.2.

4.1. Simulations set-up

In our simulations, three scenarios are designed, see Table 1. In different scenarios, different road structures are simulated. In scenario 1, all cases are studied on a three-lane homogeneous road section. The lane-drop node and the on-ramp node are studied in scenario 2 and 3, respectively. The case descriptions in Table 1 are also shown in Figure 6, which shows traffic states we expect to find.

In the first scenario, a three-lane homogeneous freeway section and two stop-and-go waves are considered: heavy congestion J_{slow} (density $\rho_{\text{slow}} =$ 400 veh/km) and light congestion J_{fast} (density $\rho_{\text{fast}} = 200$ veh/km). In case 1, the heavy congestion is in the upstream of light congestion, while

Table 1: Simulation scenarios

Scenarios	Road structures	Descriptions
1	Homogeneous road	Case 1: J_{slow} upstream of J_{fast} Case 2: J_{fast} upstream of J_{slow}
2	Lane-drop node	Case 3: After J_{slow} passing through the node, a standing queue is emerged.
3	On-ramp node	Case 4: A standing queue is emerged due to the high total demand from both of the main road and the on ramp.

in case 2, the heavy congestion is in the downstream of light congestion. Figure 6(a) and Figure 6(b) show shock wave analyses in case 1 and case 2, respectively. State 1 and 2 indicate the stop-and-go wave J_{slow} and J_{fast}, respectively. The darker shading in J_{slow} indicates a higher density than that in J_{fast}. State 3 and 4 are the downstream free-flow states of state 1 and 2, respectively. Flow in state 3 is lower than that in state 4. State 5 indicates the capacity. The shock wave analysis predicts the difference on the traffic state evolution between those two case simulations, which should be expected in our simulations. This difference indicates the importance of simulating capacity drop accurately.

To generate stop-and-go waves, we simply set the spacing profile over time of the first Lagrangian cluster. For the first Lagrangian cluster, the spacing is set to be critical spacing s_c (which is the critical spacing for a three-lane freeway) in free-flow state while the spacings in congestion are 2.5 m (in J_{slow}) and 5 m (in J_{fast}) respectively. Note that, since there are 3 lanes, 2.5 m spacing means the space is 2.5×3=7.5m.

The remaining two scenarios simulate traffic situations with nodes. In the second scenario, a lane-drop node, which connects an upstream four-lane freeway section and a three-lane freeway section, is considered. In the third scenario, the traffic model is simulated around an on-ramp node on a three-lane freeway.

In case 3, a standing queue forms at the lane-drop node after a stop-and-go wave passes through. A shock wave analysis for the case 3 is presented

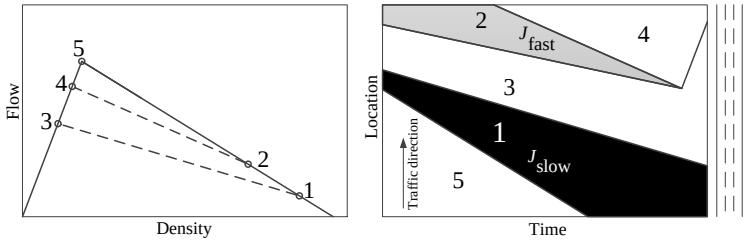

(a) Case 1: Heavy congestion J_{slow} upstream [29]

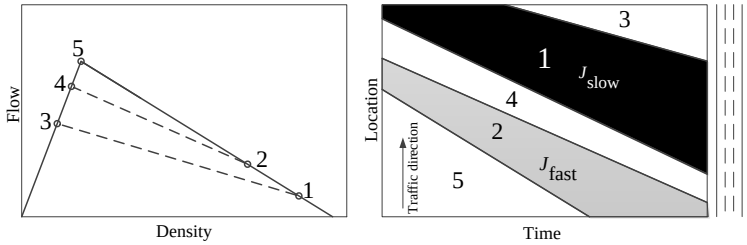

(b) Case 2:Heavy congestion J_{slow} downstream [29]

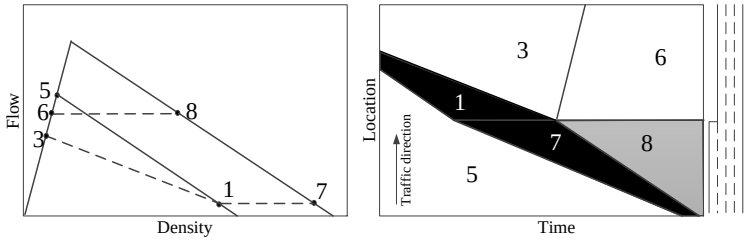

(c) Case 3: Lane-drop node scenario

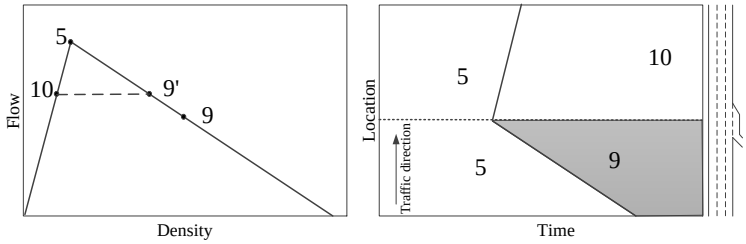

(d) Case 4: on-ramp node scenario

Figure 6: Shock wave analysis in (a) case 1, (b) case 2, (c) case 3 and (d) case 4. In each case, the left figure shows the fundamental diagram and the right one the speed/density contour

Table 2: Fundamental diagrams

Road section	Fundamental Diagram	α	q_0
3-lane section	$v_f = 114$km/h, $q_c = 6840$veh/h, $\rho_c = 60$veh/km and $w = 18$km/h	29veh/km	5000veh/h
4-lane section	$v_f = 114$km/h, $q_c = 9120$veh/h, $\rho_c = 80$veh/km and $w = 18$km/h	39veh/km	6667veh/h
On ramp	$v_f = 114$km/h, $q_c = 2280$veh/h, $\rho_c = 20$veh/km and $w = 18$km/h	N/A	N/A

in Figure 6(c). The stop-and-go wave J_{slow} is shown as state 1. The downstream state of J_{slow} is state 3. A standing queue is state 8, whose queue discharge rate is shown as state 6. A shock wave between state 3 and state 6 is expected to distinguish different queue discharge rates of different queues. In case 4, a standing queue (shown as state 9 in Figure 6(d)) forms when the on-ramp flow enter into the main road where the density has already reached a critical density. The shock wave analyses for case 4 is shown in Figure 6(d). The studied cases around nodes in this paper have been empirically observed in [4] and [35]. Because empirical observations in [4] and [35] show different congested states at lane-drop and on-ramp bottleneck, this work uses different number (state 8 and state 9) to denote the congested state of the standing queue forming at lane-drop and on-ramp bottleneck, respectively. In Case 4, the on ramp is one-lane and the merging ratio $\gamma = 0.35$. In both of case 3 and case 4, the nodes are located at $x = 0$ m.

In all cases, at the beginning of simulations ($t = 0$ s), the spacing of all Lagrangian clusters on the main road are set to be s_c.

The fundamental diagrams in our simulations are summarized in Table 2. For simplicity, the capacity drop is not incorporated when modeling Lagrangian clusters on the on-ramp section. In all cases, $\Delta N = 1$, which make each Lagrangian cluster can be seen as a vehicle. It is worthwhile to notice that we also can set $\Delta N > 1$ which will make the new model a macroscopic

model. To ensure the stability, this paper sets Δt following (13):

$$\Delta t \approx \begin{cases} 0.45s, & \text{in scenario 1} \quad (18) \\ 0.34s, & \text{in scenario 2} \quad (19) \\ 0.45s, & \text{in scenario 3} \quad (20) \end{cases}$$

4.2. Simulations results

When simulating in Lagrangian coordinates, we can draw the trajectories of each Lagrangian cluster, as presented in Figure 7. A space contour plot (see Figure 8 and Figure 9(a)) shows different traffic states in space-time. The simulation results all fit the expectations shown in Figure 6.

In Figure 7, the blue lines are the Lagrangian clusters. The queue discharge rate of J_{slow} is 5052 veh/h (capacity drop = 26%) and that of J_{fast} is 5626 veh/h (capacity drop = 18%). In Case 1, the queue length of J_{slow} increases while the jam J_{fast} diminishes. That is because for J_{slow} the inflow (equals to capacity) is higher than the outflow (i.e., the definition of capacity drop), while the queue discharge rate of J_{fast} is lower than the inflow which is the outflow of J_{slow}. In case 2 both of queues grow because the queue discharge rates of both jams are lower than their inflows. If we assume that the first Lagrangian cluster in Figure 7 decelerate because of a speed limit, and that the first cluster is the last cluster under the control of the speed limit, the traffic state transitions given in Figure 7 present impacts of the speed limit on the upstream road traffic. Without considering instabilities, a lower speed limit can result in a more congested traffic state J_{slow} which will be more difficult to be dissolved because its queue discharge rate is lower, by contrast to J_{fast}. The simulation results in Figure 7 is the same as expected in Figure 6(a) and Figure 6(b).

The simulation results in case 3 are shown in the spacing contour plot in Figure 8. The spacing decreases as the color goes darker, see the legend in Figure 8. It is shown that as a stop-and-go wave passes the lane-drop node, a standing queue forms. In Figure 8, The congestion is shown as dark colour. In the downstream of congestion, a dashed line distinguishes the state downstream of the stop-and-go wave and the one downstream of the standing queue. The shock wave shown as dashed line has been expected in Figure 6(c). Note that, this shock wave has been frequently observed on freeways, see [4] and [35].

Finally, Figure 9 shows the simulation results on an on-ramp node. Figure 9(a) shows the spacing contour. To better understand the model, the

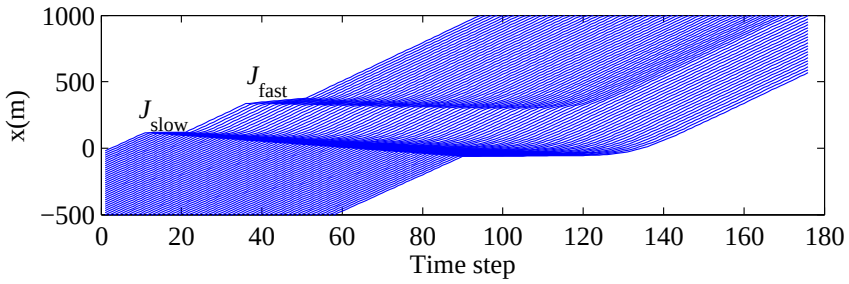

(a) Case 1: Low-speed jam J_{slow} upstream

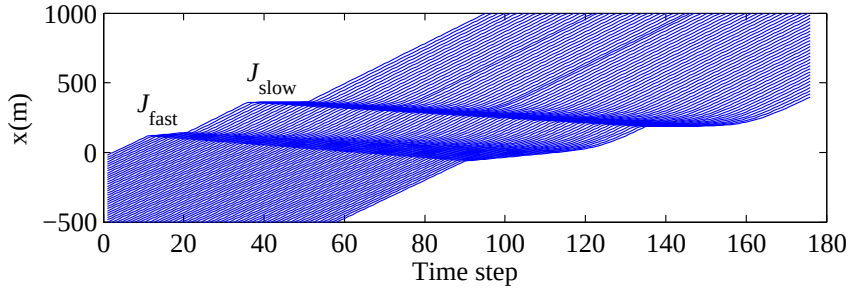

(b) Case 2: Low-speed jam J_{slow} downstream

Figure 7: Simulation results in (a) case 1 and (b) case 2 in Lagrangian coordinates [29]

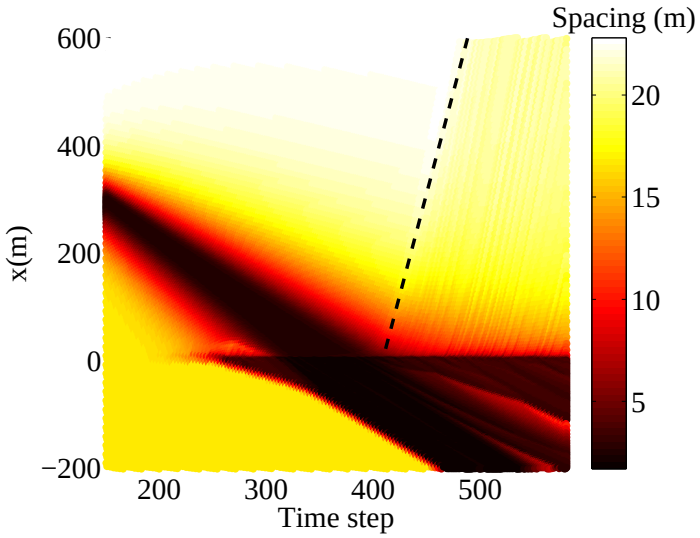

Figure 8: Spacing contour in case 3: simulations around a lane-drop node

trajectories of clusters from both of main road and the on ramp in a rectangle area (highlighted by a blue rectangle) in Figure 9(a) are shown in Figure 9(b), where the dashed lines are the trajectories of on-ramp clusters while the solid ones are the clusters from the main road. Around time step 60, the first Lagrangian cluster merges into the main road. A standing queue begins forming from that time. In Figure 9(a), before the merging of the first Lagrangian cluster from the on ramp, the spacing between clusters are critical spacing shown as orange. Since the onset of a standing queue, in the downstream of the standing queue, the spacing between Lagrangian clusters are larger than the critical spacing.

It is noticed that every time when a Lagrangian cluster passes the bottleneck, the spacing distributed to those clusters can be different, that results in different congested states in the upstream of bottlenecks. As shown in Figure 7, the sequence of Jfast and J_{slow} on links can influence the traffic state transition. So it is shown in Figure 8 and Figure 9 that different traffic state transitions can appear. With a same simulation set-up, the simulation results are the same no matter how many times the simulation is run, which means the model is deterministic.

In summary, our model works when reproducing the capacity drop and the relation between the congestion and its queue discharge rate.

5. Conclusion

This paper presents a new kinematic wave model incorporating the capacity drop phenomenon to improve the validity and applicability of the classical kinematic wave model. It is solved in Lagrangian coordinates with an upwind scheme for its simplicity and high accuracy. The simplicity due to that the traffic character propagates only in one-direction to followers in Lagrangian coordinates. The high accuracy is shown as smaller numerical errors. This means that the Lagrangian kinematic wave model gives efficient simulations.

This new model uses predefined hysteresis loops to capture the capacity drop – clockwise in Eurlerian coordinates and counter clockwise in Lagrangian coordinates. The loop is determined by an empirical relation between the speed in congestion and the queue discharge rate. In contrast to other first order models, it can reproduce the capacity drop and its important features, such as the relation between the speed in congestion and the queue discharge rate. The model is applied to jams on both of a homogeneous road

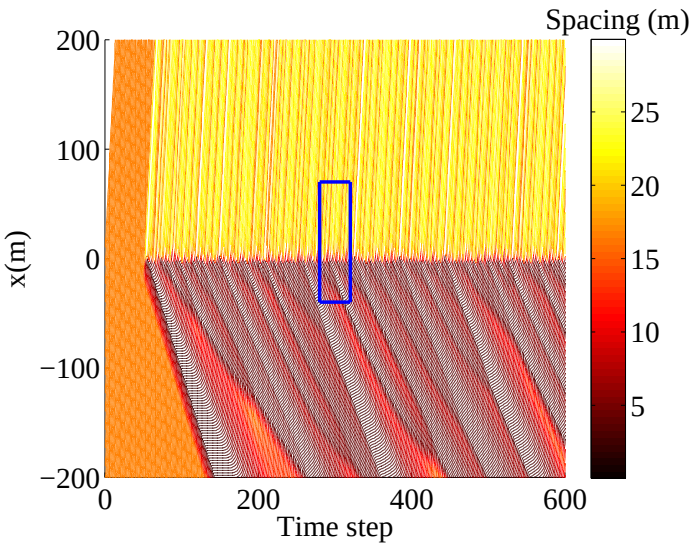

(a) Spacing contour in case 4: simulations around an on-ramp node

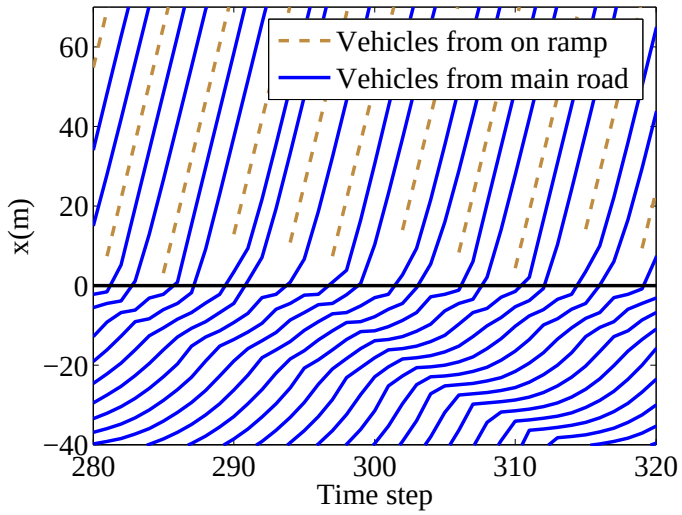

(b) Trajectories of Lagrangian clusters in case 4: simulations around an on-ramp node

Figure 9: Simulation results in case 4 is shown as (a) spacing contour and (b) trajectories of Lagrangian clusters

section and nodes (including lane-drop and on-ramp nodes) in this paper, which means the model can be applied to a traffic network.

The Lagrangian kinematic wave model is suitable for traffic applications, such as traffic state estimations, traffic delay calculations and model based dynamic traffic management. The Lagrangian kinematic wave model can contribute to accurate knowledge of accumulated vehicles by providing accurate capacity drop magnitude, which benefits traffic state estimations and traffic delays calculations greatly. The increasing accurate knowledge of the traffic system benefits active traffic management. For locations with speed limits and ramp meter installations, the dynamic speed limit and ramp metering rate can be more precise and situation-oriented. For modeling speed limits, we can revise the fundamental spacing-speed relation by reducing the free-flow speed in the new model. Note that, in the upstream of the speed limited road section, a stop-and-go wave might forms if the upstream demand is high enough. Our model can give accurate capacity drop for this stop-and-go wave, which is relevant for evaluating the speed limit consequences and determining the dynamic speed limit values.

Acknowledgement

This research is financially supported by China Scholarship Council (CSC) and the NWO grant "There is plenty of room in the other lane".

[1] K. Hall, Fred L. Agyemang-Duah, Freeway capacity drop and the definition of capacity, Transportation Research Record (1320) (1991) 91–98.

[2] J. H. Banks, Two-capacity phenomenon at freeway bottlenecks: A basis for ramp metering?, Transportation Research Board (1320) (1991) 83–90.

[3] M. Papageorgiou, Some remarks on macroscopic traffic flow modelling, Transportation Research Part A: Policy and Practice 32 (5) (1998) 323 – 329.

[4] K. Yuan, V. L. Knoop, S. P. Hoogendoorn, Capapcity drop: relation between speed in congesiton and the queue discharge rate, Transportation Research Record 2491 (2015) 72–80.

[5] K. Yuan, V. L. Knoop, S. P. Hoogendoorn, A microscopic investigation into the capacity drop: Impacts of the bounded acceleration and reaction

time, in: Proceedings of the 95th Annual Meeting of the Transportation Reseach Board, Washington D.C., 2016.

[6] S. P. Hoogendoorn, P. H. Bovy, State-of-the-art of vehicular traffic flow modelling, Journal of Systems and Control Engineering 215 (4) (2001) 283–303.

[7] A. Kotsialos, M. Papageorgiou, C. Diakaki, Y. Pavlis, F. Middelham, Traffic flow modeling of large-scale motorway networks using the macroscopic modeling tool METANET, Intelligent Transportation Systems, IEEE Transactions on 3 (4) (2002) 282–292.

[8] A. Hegyi, B. D. Schutter, H. Hellendoorn, Model predictive control for optimal coordination of ramp metering and variable speed limits, Transportation Research Part C 13 (3) (2005) 185–209.

[9] C. F. Daganzo, Requiem for second-order fluid approximations of traffic flow, Transportation Research Part B: Methodological 29 (4) (1995) 277 – 286.

[10] Y. Lu, S. C. Wong, M. Zhang, C.-W. Shu, The entropy solutions for the lighthill-whitham-richards traffic flow model with a discontinuous flow-density relationship, Transportation Science 43 (4) (2009) 511–530.

[11] W.-L. Jin, Q.-J. Gan, J.-P. Lebacque, A kinematic wave theory of capacity drop, Transportation Research Part B: Methodological 81 (2015) 316 – 329.

[12] M. J. Cassidy, Bivariate relations in nearly stationary highway traffic, Transportation Research Part B: Methodological 32 (1) (1998) 49 – 59.

[13] T. J. Maria, F. Soriguera, N. Geroliminis, Coordinated active traffic management freeway strategies using capacity-lagged cell transmission model, in: Proceedings of the 93rd Annual Meeting of the Transportation Research Board (TRB), Washington DC, 2014.

[14] A. Srivastava, N. Geroliminis, Empirical observations of capacity drop in freeway merges with ramp control and integration in a first-order model, Transportation Research Part C: Emerging Technologies 30 (0) (2013) 161 – 177.

[15] L. Alvarez-Icaza, G. Islas, Hysteretic cell transmission model, in: Intelligent Transportation Systems - (ITSC), 2013 16th International IEEE Conference on, 2013, pp. 578–583.

[16] J. Lebacque, A two phase extension of the lwr model based on the boun-bounded of traffic acceleration, in: Proceedings of the 15th international symposium on transportation and traffic theory (ISTTT), South Australia, 2002.

[17] J. Lebacque, Two-phase bounded-acceleration traffic flow model: Analytical solutions and applications, Transportation Research Record: Journal of the Transportation Research Board 1852 (2003a) 220–230.

[18] J. Lebacque, Traffic and Granular Flow, Springer Berlin Heidelberg, Berlin, Heidelberg, 2003b, Ch. Intersection Modeling, Application to Macroscopic Network Traffic Flow Models and Traffic Management, pp. 261–278.

[19] M. Khoshyaran, J. Lebacque, Capacity drop and traffic hysteresis as a consequence of bounded acceleration, IFAC-PapersOnLine 48 (1) (2015) 766 – 771, 8th Vienna International Conferenceon Mathematical ModellingMATHMOD 2015.

[20] T. Monamy, H. Haj-Salem, J.-P. Lebacque, A macroscopic node model related to capacity drop, Procedia - Social and Behavioral Sciences 54 (0) (2012) 1388 – 1396, proceedings of {EWGT2012} - 15th Meeting of the {EURO} Working Group on Transportation, September 2012, Paris.

[21] A. Muralidharan, R. Horowitz, Computationally efficient model predictive control of freeway networks, Transportation Research Part C: Emerging Technologies 58, Part C (2015) 532 – 553, special Issue: Advanced Road Traffic Control.

[22] C. Roncoli, M. Papageorgiou, I. Papamichail, Traffic flow optimisation in presence of vehicle automation and communication systems - part i A first-order multi-lane model for motorway traffic, Transportation Research Part C: Emerging Technologies 57 (2015) 241 – 259.

[23] A. Srivastava, W. Jin, A lane changing cell transmission model for modeling capacity drop at lane drop bottlenecks, in: Proceedings of the 95th

Annual Meeting of the Transportation Research Board (TRB), Washington DC, 2016.

[24] M. Kontorinaki, A. Spiliopoulou, C. Roncoli, M. Papageorgiou, Capacity drop in first-order traffic flow models: Overview and real-data validation, in: Proceedings of the 95th Annual Meeting of the Transportation Research Board (TRB), 2016, paper no. 16-3541.

[25] J. Treiterer, J. Myers, The hysteresis phenomenon in traffic flow, Transportation and traffic theory 6 (1974) 13–38.

[26] H. Deng, H. M. Zhang, On traffic relaxation, anticipation, and hysteresis, Transportation Research Record: Journal of the Transportation Research Board 2491 (2015) 90–97.

[27] J. A. Laval, Hysteresis in traffic flow revisited: An improved measurement method, Transportation Research Part B: Methodological 45 (2) (2011) 385 – 391.

[28] Y. Yuan, J. van Lint, R. Wilson, F. van Wageningen-Kessels, S. Hoogendoorn, Real-time lagrangian traffic state estimator for freeways, Intelligent Transportation Systems, IEEE Transactions on 13 (1) (2012) 59–70.

[29] K. Yuan, V. L. Knoop, T. Schreiter, S. P. Hoogendoorn, A hybrid kinematic wave model incorporating capacity drops, in: Intelligent Transportation Systems (ITSC), 2015 18th International IEEE Conference on, 2015.

[30] F. van Wageningen-Kessels, Multi-class continuum traffic flow model: Analysis and simulation methods, Ph.D. thesis, Delft University of Technology (2013).

[31] L. Leclercq, J. A. Laval, E. Chevallier, The lagrangian coordinates and what it means for first order traffic flow models, in: M. B. B Heydecker, R. Allsop (Eds.), 17th International Symposium on Transportation and Traffic Theory (ISTTT), Elsevier, New York, 2007.

[32] L. Leclercq, Hybrid approaches to the solutions of the "Lighthill-Whitham-Richards" model, Transportation Research Part B: Methodological 41 (7) (2007) 701 – 709.

[33] D. Helbing, M. Treiber, Numerical simulation of macroscopic traffic equations, Computing in Science and Engineering 1 (5) (1999) 89–99.

[34] F. van Wageningen-Kessels, Y. Yuan, S. P. Hoogendoorn, H. van Lint, K. Vuik, Discontinuities in the lagrangian formulation of the kinematic wave model, Transportation Research Part C: Emerging Technologies 34 (2013) 148 – 161.

[35] K. Yuan, V. L. Knoop, L. Leclercq, S. P. Hoogendoorn, Capacity drop: A comparison between stop-and-go wave and standing queue at lane-drop bottleneck, in: 2014 Traffic Flow Theory Summer meeting, Portland, 2014.